HardwareX 14 (2023) e00420

Contents lists available at ScienceDirect

HardwareX

journal homepage: www.elsevier.com/locate/ohx

Hardware Article

A handheld plug-and-play microfluidic liquid handling automation platform for immunoassays

Sheng Wang, Baichen Li, David McLeod, Zhenyu Li *

Department of Biomedical Engineering, The George Washington University, 800 22nd Street, NW, Washington, DC 20052, USA

ARTICLE INFO

Article history:
Received 31 October 2022
Received in revised form 28 March 2023
Accepted 10 April 2023

Keywords:
Microfluidics
Lab-on-a-chip
Automation
Handheld
Immunoassay
Liquid handling
Plug-and-play
Point-of-care diagnostics

ABSTRACT

Lab-on-a-chip technologies and microfluidics have pushed miniaturized liquid handling to unprecedented precision, integration, and automation, which improved the reaction efficiency of immunoassays. However, most microfluidic immunoassay systems still require bulky infrastructures, such as external pressure sources, pneumatic systems, and complex manual tubing and interface connections. Such requirements prevent plug-and-play operation at the point-of-care (POC) settings. Here we present a fully automated handheld general microfluidic liquid handling automation platform with a plug-and-play 'clamshell-style' cartridge socket, a miniature electro-pneumatic controller, and injection-moldable plastic cartridges. The system achieved multi-reagent switching, metering, and timing control on the valveless cartridge using electro-pneumatic pressure control. As a demonstration, a SARS-CoV-2 spike antibody sandwich fluorescent immunoassay (FIA) liquid handling was performed on an acrylic cartridge without human intervention after sample introduction. A fluorescence microscope was used to analyze the result. The assay showed a limit of detection at 31.1 ng/mL, comparable to some previously reported enzyme-linked immunosorbent assays (ELISA). In addition to automated liquid handling on the cartridge, the system can operate as a 6-port pressure source for external microfluidic chips. A rechargeable battery with a 12 V 3000 mAh capacity can power the system for 42 h. The footprint of the system is 16.5 × 10.5 × 7 cm, and the weight is 801 g, including the battery. The system can find many other POC and research applications requiring complex liquid manipulation, such as molecular diagnostics, cell analysis, and on-demand biomanufacturing.

Specifications table

Hardware name	Handheld plug-and-play microfluidic liquid handling automation platform
Subject area	• Biological science (e.g., Microbiology and Biochemistry)
Hardware type	• Biological sample handling and preparation

(*continued on next page*)

* Corresponding author.
E-mail address: zhenyu@gwu.edu (Z. Li).

https://doi.org/10.1016/j.ohx.2023.e00420
2468-0672/

(*continued*)

Hardware name	Handheld plug-and-play microfluidic liquid handling automation platform
Closest commercial analog	Elveflow OB1 MK3+ Microfluidic flow controller
Open source license	GPLv3
Cost of hardware	$1395
Source file repository	https://doi.org/10.17632/mxr5zkg5fx.2

Hardware in context

The highly selective antigen–antibody interaction makes immunoassay a powerful analytical technique in clinical testing and biomedical research [1,2]. Typical immunoassay experiments that provide highly sensitive and accurate quantitative results, such as Enzyme-Linked Immunosorbent Assay (ELISA), require extensive liquid handling operations [3]. Traditional robotic pipetting systems have been developed for high throughput and fully automated operations, which cost tens of thousands of dollars (e.g., Opentrons, Parker's automation) [4,5]. However, their sizes, weights, and power requirements make them only available in benchtop or larger form factors. With the development of microfluidic technology, numerous efforts have been put into combining it with immunoassay systems. With on-chip pumps and valves based on MEMS and elastomeric (e.g., Polydimethylsiloxane (PDMS)) technologies, the sizes of the liquid handling subsystems (cartridges and chips) are greatly reduced to centimeter scale [6–10]. The liquid manipulation resolution and accuracy are also improved by orders of magnitude [11,12]. However, most current microfluidic setups still require bulky off-chip infrastructures such as pressure sources, pneumatic controllers, and electronics, which often lead to non-portable systems. In addition, such PMDS chip-based systems still rely on manual tubing connections, pressure source setup, and external sample reservoir connection. Even some self-claimed automated systems cannot avoid all the hands-on steps, which makes plug-and-play operation almost impossible for such microfluidic platforms [13–18]. Despite systems with the goal of being plug-and-play have been developed, several important functionalities of microfluidic systems were compromised (e.g., precise pressure regulation, parallel reagent control, and repeatable reagent switching), which limits the scope of application [19]. Moreover, the fabrication processes of the chips/cartridges for the abovementioned systems require complex steps and equipment, which results in high costs and lengthy turn-around times between conception and prototypes.

In this work, we demonstrate a fully automated plug-and-play handheld platform for liquid handling in generic microfluidic immunoassays, featuring a 'clamshell-style' cartridge-manifold interfacing socket, a miniature electro-pneumatic controller, and disposable plastic cartridges (Fig. 1). With the flexibility of 3 programmable dynamic/stable pressure outputs and 6 parallel liquid manipulation lines, the system can achieve multi-reagent switching, metering, and timing control on a valveless cartridge for assays with up to 6 reagents. The system exempts the end-user from tubing/needle/chip connection and other setups, allowing a plug-and-play simplicity without sacrificing the merits of microfluidics-based immunoassays.

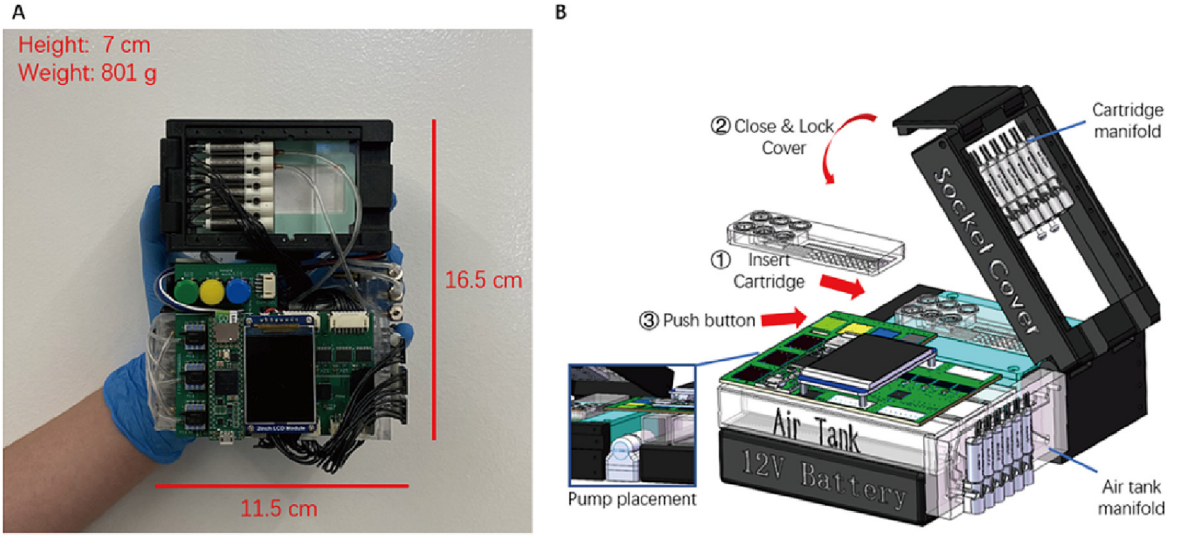

Fig. 1. (A) Picture of the handheld system. The footprint is 16.5 × 11.5 × 7 cm. (B) The drawing of the system shows the operation of a plug & play assay. Inset: The expanded view shows the pump is located under the PCB, between the clamshell socket and the battery. A 3-step operation after sample loading could start the assay and let it proceed automatically.

In addition to the sample cartridge for automated assay conduction, an adapter cartridge was also demonstrated, which turns the system into a six-port pressure source for general microfluidic applications. The cartridges could be manufactured by one-step injection molding, which allows mass production hence reducing the cost of each test.

The function of this system could be exploited with different cartridge/manifold designs and integration with other devices, such as readout sensors, heating/cooling systems, and wireless communication modules, through the abundant power and signal interfaces on the system. With a 12 V 3000 mAh battery, the system can run continuously for 42 h (the demonstrated assay) after a full charge. The footprint of this system is 16.5 × 11.5 × 7 cm (L × W × H), and the weight is 801 g (battery included).

Hardware description

Fig. 1 (B) shows the layout and the operation procedure of the system for an automated operation. Except for automated execution of the pre-loaded commands in the microSD card, the system can also be controlled via real-time commands through a USB connection. The handheld assay system consists of three subsystems: (1) a pneumatic subsystem with a diaphragm pump, three air tanks, and an air tank manifold for the generation and control of three pressure levels; (2) a microfluidic subsystem with a clamshell-style socket structure, a microfluidic cartridge, and a cartridge manifold; (3) an electronic subsystem with a Teensy 4.1 development board, barometric sensors, IO expansion devices, liquid crystal display (LCD), and power driver devices on a printed circuit board (PCB).

The block diagram of the system is shown in Fig. 2. Detailed descriptions of each subsystem are illustrated in subsequent sections.

Pneumatic subsystem

As shown in Fig. 2, the pneumatic subsystem provides three programmable pressure levels (P1, P2, P3) from three air tanks by utilizing a 4.5 V diaphragm pump, solenoid valves, and an air tank manifold. Each of these pressures could be set and adjusted individually throughout the assay process. The output port and input port of the miniature pump are connected to air tank 1 and air tank 3 to deliver and extract air correspondingly. The pressure stored in air tank 2 is gathered from air tank 1. And the pressure stored in air tank 2 is also used to increase the pressure in air tank 3. P1 can range from 0 to 5.8 psi (39.98 kPa) and provide a buffer for the precise pressure output P2. P2 can range from 0 psi to the level of P1 to drive the reagents. P3 can range from −5.8 psi (-39.98 kPa) to the level of P2. The negative P3 pressure output makes reversible

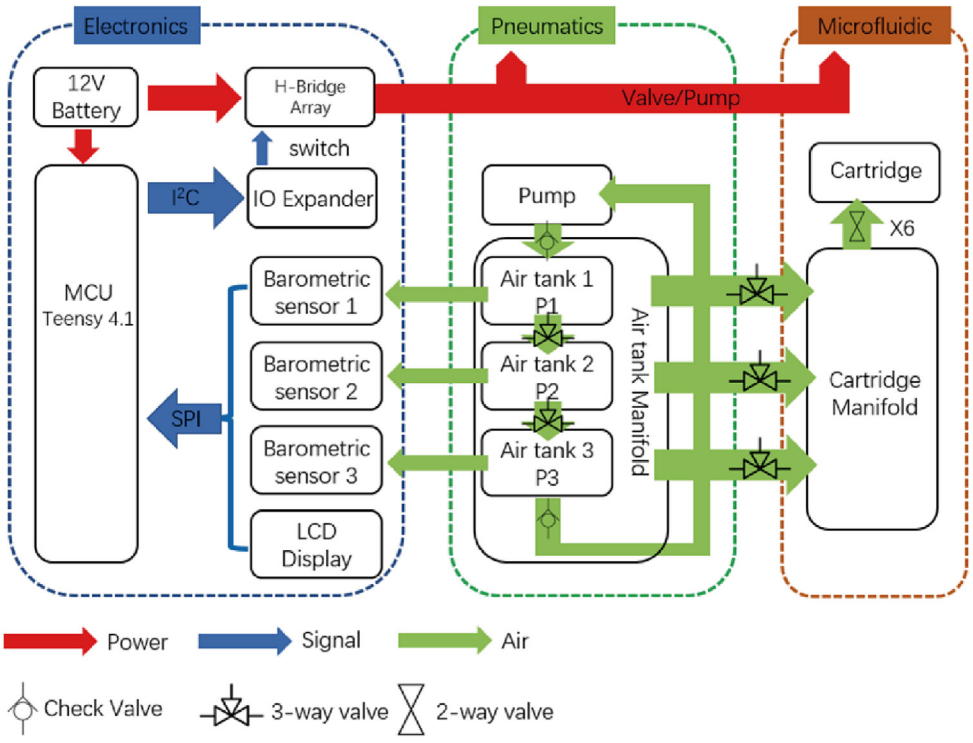

Fig. 2. Block diagram of the system. The system consists of electronics, pneumatics, and microfluidic subsystem. The system is powered by a 12 V battery and can provide three output pressure to drive multiple reagents. Detailed explanations of the subsystems are given in the main text.

flow possible. Although the achieved pressure levels are sufficient for liquid driving in microfluidic channels, higher pressure could be achieved with a more powerful pump to expand the liquid handling capability [6,20,21]. The air tanks are made of acrylic tubes that are 110 mm long and 19 mm wide and high. A brass barbed connector is screwed on top of each air tank and connected to the corresponding barometric sensor through silicone tubing. One side of the air tank is sealed, and the other side is connected to the air tank manifold that has six 3-port (A, B, Common) solenoid latching valves for pressure stabilizing and output (Fig. 3).

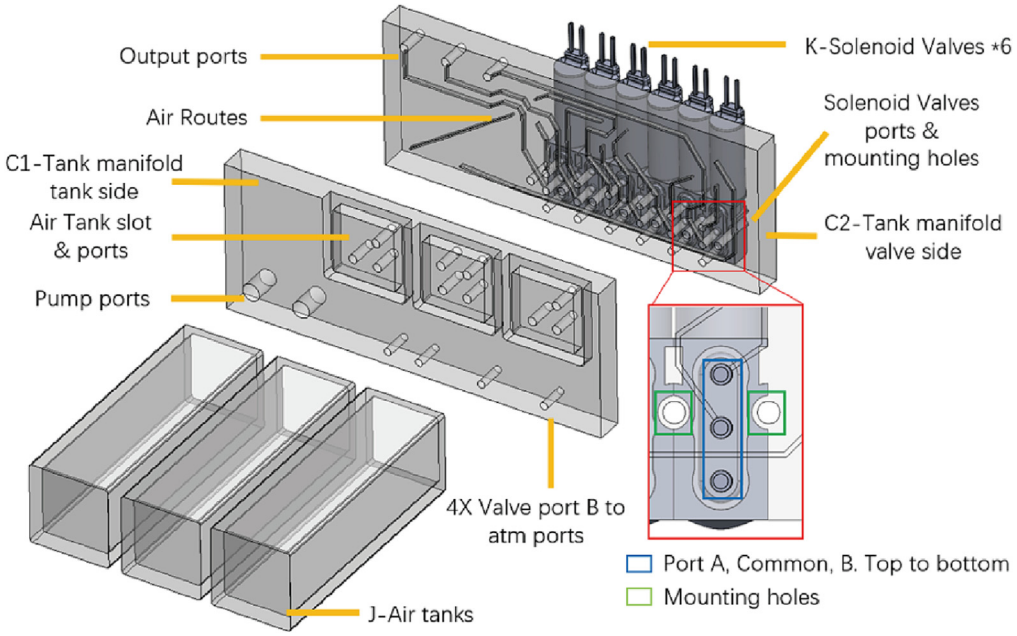

Fig. 3. Demonstration of the pneumatic subsystem. Three air tanks and six solenoid valves are glued and mounted on the two-layer diffusion bonded manifold. The pump ports and output ports are tapped and fitted with barbed connectors and elbow connectors, then connected to silicone tubing. The magnified box shows the ports for solenoid valves on the manifold. The mounting holes are tapped to fit 2–56 screws to mount the solenoid valves.

Microfluidic subsystem

The handheld system is designed for a plug-and-play cartridge method. A clamp structure is utilized to immobilize the cartridge, align the cartridge and cartridge manifold, and provide a hermetically sealed environment (Fig. 4). The cartridge manifold is designed in a similar method to the air tank manifold, with two pieces of acrylic. A slot is machined out at the bottom of the cartridge manifold to accommodate the elastomer gasket, the cylinders with air output ports in the middle will be aligned to the reagent reservoirs' positions across the gasket (Fig. 4. C). The spring stage will be pressed down after the cover is closed and locked. The cartridge will be pushed to the cartridge manifold and elastomer gasket by the force of springs, thus keeping the O-ring, gasket, and cartridge manifold in contact firmly and preventing air leakage. The compressed air and vacuum in the three air tanks can be delivered to the reagent reservoirs to drive the reagents down to the channels through the vertical via holes by connecting silicone tubing from the output ports on the air tank manifold to the input ports on cartridge manifold. In the sample cartridge manifold, 6 solenoid valves are mounted to control the air output ports. The common port of each solenoid valve is connected to the air output ports, while the port A is sealed, and the port B is connected to the air input ports. Each output port could be controlled individually.

Instead of implementing the Quake-style valves used in multi-layer PDMS elastomeric microfluidic devices, we achieve liquid switching, metering, and timing control functionality on a simple single-layer valveless cartridge by selectively cutting off and sealing the reagent driving pressure in the cartridge manifold through the solenoid valves on it [6]. Only the channel carrying the desired reagent for the current step is pressurized. Also, the pressures needed to flow the reagents are reduced to less than 2 psi (13.79 kPa). This allows us to use a low-power 4.5 V miniature pump and low pump activation frequency to achieve the desired functionality with reduced power consumption and cost.

Electronic subsystem

The electronic subsystem is based on a Teensy 4.1 development board that features an ARM Cortex-M7 processor. The following tasks are carried out by the firmware programmed in the board: (1) Execute the command script that is pre-

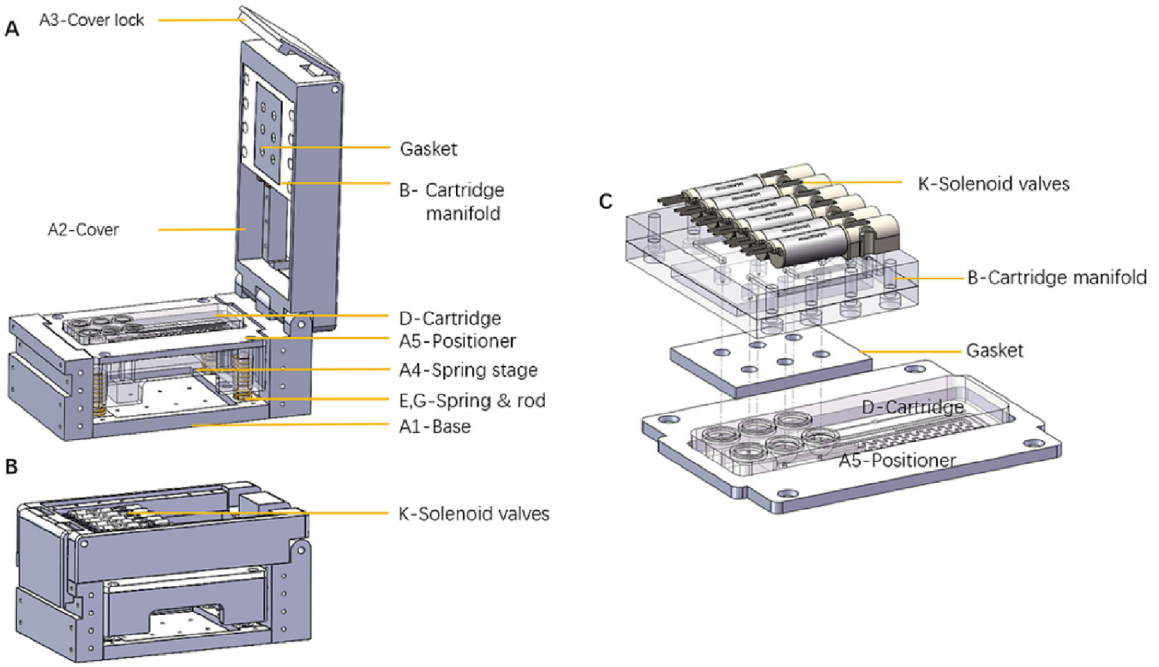

Fig. 4. Clamshell socket structure designed for cartridge plug-and-play operation, including immobilization, alignment, and air seal. (A) Cover unlocked, the spring stage is supported by the springs under it. (B) Cover locked, the spring stage is pressed down. Air seal achieved. (C) Alignment of the cartridge manifold, gasket, cartridge, and positioner. The gasket will be squeezed by force from springs to achieve an air seal once the cover is locked. The pressure will be delivered to the reagent reservoirs.

loaded in the microSD card or received from a computer, (2) Receive data from the three barometric sensors, (3) Adjust and stabilize pressures in three air tanks with IO expansion chips (Diodes Incorporated PI4IOE5) and H-bridge drivers (Toshiba TB6612FNG), (4) display and store pressure and assay information on the LCD and microSD card. The firmware works following a tick method to execute the above-mentioned tasks every 30 ms. Three pressure readings are retrieved from the sensors through the SPI interface at the beginning of each tick. Two IO expansion chips' inputs are connected to two I^2C interfaces on the board to expand the I^2C ports to 96 GPIO, and the output ports of IO expanders are connected to 10 H-bridge chips' input ports to control up to 20 solenoid valves or pumps. The on/off status of the pump, solenoid valves on the two manifolds will be updated through the I^2C protocol by comparing the pressure readings and the target pressures set by the user. After these functions are done, pressure readings, current assay procedure, and operation notice will be uploaded to the 2-inch LCD through a second SPI interface.

The electrical subsystem is powered by a 3000 mAh power bank with 12 V and USB output capability. The USB output port is connected to the Teensy 4.1 board and provides a 5 V and 3.3 V power rail for the barometric sensors, IO expanders, and signal rails of the H-bridges. The power rails of H-bridge chips could be selectively connected to 12 V or 5 V output individually to supply the solenoid valves and diaphragm pump. A 5 V voltage regulator on the PCB can also be used to supply the Teensy board and aforementioned components through the 12 V rail. Several extra power rails are provided to allow external power sources connection for component compatibility and system customizability.

The proposed hardware provides several advantages:

- Plug-and-play automation ease is offered without compromising the important functionalities and merits of microfluidic systems.
- Sample immunoassay on a cartridge offer sensitivity and accuracy comparable to some previously reported ELISA conducted on standard 96-well plates.
- Thermoplastic cartridges are compatible with surface functionalization for diverse assay types.
- One-layer cartridge design compatible with injection molding fabrication reducing the cost per test.
- Modular design and additional power/signal interfaces allow modifications and extensions for different applications in POC and research circumstances.
- The compact size, lightweight, and battery make the system suitable for various working situations.

Design files summary

Design file name	File type	Open source license	Location of the file
A1-Base	STL	GPLv3	https://doi.org/10.17632/mxr5zkg5fx.2
A2-Cover	STL	GPLv3	https://doi.org/10.17632/mxr5zkg5fx.2
A3-Cover lock	STL	GPLv3	https://doi.org/10.17632/mxr5zkg5fx.2
A4-SpringStage	STL	GPLv3	https://doi.org/10.17632/mxr5zkg5fx.2
A5-Positioner	STL	GPLv3	https://doi.org/10.17632/mxr5zkg5fx.2
B1-Cartridge_manifold_top	STEP	GPLv3	https://doi.org/10.17632/mxr5zkg5fx.2
B2-Cartridge_manifold_bottom	STEP	GPLv3	https://doi.org/10.17632/mxr5zkg5fx.2
C1-Tank_manifold_tank	STEP	GPLv3	https://doi.org/10.17632/mxr5zkg5fx.2
C2-Tank_manifold_valve	STEP	GPLv3	https://doi.org/10.17632/mxr5zkg5fx.2
D1-Assay_cartridge	STEP	GPLv3	https://doi.org/10.17632/mxr5zkg5fx.2
D2-Adapter_cartridge	STEP	GPLv3	https://doi.org/10.17632/mxr5zkg5fx.2
Board.zip	sch and brd	GPLv3	10.17632/mxr5zkg5fx.2
Firmware	ZIP	GPLv3	https://doi.org/10.17632/mxr5zkg5fx.2
ElectronicsBOM	CSV	GPLv3	10.17632/mxr5zkg5fx.2
SampleLua	Lua	GPLv3	10.17632/mxr5zkg5fx.2

The STL and STEP folders contain the 3D printed and CNC machined parts, respectively. The Board.zip file contains the schematic and board layout for the PCB. The ElectronicsBOM.csv file records the electronic components on the PCB board, excludes the Teensy board, button, JST connectors, and pressure sensors.

The firmware.zip should be extracted and opened through the PlatformIO extension in Visual Studio Code software to program the Teensy board. The sample Lua script was used for the sample SARS-CoV-2 assay. Detailed function explanation can be found in Firmware/lib/LuaExt/src/CustomLib.cpp.

Bill of materials summary

Designator	Component	Number	Cost per unit – currency	Total cost – currency	Source of materials	Material type
3D printing filament	Z-Ultrat	1	$59	$59	Zortrax	Polymer
E-Spring	Die spring	1	$5.35	$5.35	Amazon	Metal
F-3 mm rod	3 mm rod	1*	$5.49	$5.49	Amazon	Metal
G-4 mm rod	4 mm rod	1*	$5.49	$5.49	Amazon	Metal
H-Flat Screw	2–56 screw	1*	$8.87	$8.87	McMaster	Metal
I-Self-tapping screw	2–28 self-tapping screw	1*	$4.88	$4.88	Amazon	Metal
Teensy	Teensy 4.1	1	$37.5	$37.5	Amazon	Semiconductor/ Other
PCB	Mainboard	1	$8	$8	JLCPCB	Semiconductor/ Other
Electronic components	Electronic components on PCB*	1**	$35	$35	Digikey	Semiconductor/ Other
LCD Display	Waveshare 2 in. LCD	1	$14.75	$14.74	Amazon	Semiconductor/ Other
Pressure sensor	Pressure sensor	3	$62.6	$187.8	Digikey	Other
Button	Push button switch kit	1	$8.99	$8.99	Amazon	Other
JST Connectors	Wire connectors on PCB	1	$18.99	$18.99	Amazon	Other
B-Cartridge manifold/C-Air tank manifold	Acrylic sheet	1	$18.38	$18.38	McMaster	Polymer

(*continued*)

Designator	Component	Number	Cost per unit – currency	Total cost – currency	Source of materials	Material type
J-Air tank	Acrylic Tube	1	$6.8	$6.8	McMaster	Polymer
K-Solenoid valve	LHLA1221111H	12	$71.05	$852.6	Lee.co	Other
L-Check Valve	3/16'' Check valve	1	$2.5	$2.5	Amazon	Other
M−Pump	Boxer pump 22000.011	1	€49.83	€49.83	Boxer	Other
Fitting connector 1	EB25 fitting	2	$1.91	$3.82	Pneumadyne	Metal
Fitting connector 2	EA-LB10-SLOT fitting	3	$5.27	$15.81	Pneumadyne	Metal
Fitting connector 3	3–56 to 1/16'' fitting	5	$0.51	$2.55	Airengr	Metal
Tubing 1	3/32'' ID tubing	1*	$7.99	$7.99	Amazon	Other
Tubing 2	1/16'' ID tubing	1*	$5.49	$5.49	Amazon	Other
12 V battery	12 V battery	1	$28.79	$28.79	Amazon	Other

*Sold in bulk, actual cost should be less.

**Please see electronicBOM.csv for detailed BOM of electronic components on PCB.

Build instructions

Pre-assembly

PCB soldering

Solder the electronic components and pressure sensors to the PCB with a soldering iron per the layout in the board file.

3D printing

The clamping structures require 3D-printed parts. These parts were printed with Z-Ultrat filament using a Zortrax M200 printer, with the default settings in the Zortrax software. Print all the parts in the STL folder for assembly.

Laser cutting (optional)

Cut the acrylic sheet into stocks in the appropriate sizes (please refer to CAD files) using a laser engraver (Universal Laser System) for computer numerical control (CNC) milling and air tank bottom sealing. The 65 W CO2 laser's movement speed in the cutting program (UCP) should be set to 0.6% of its maximum speed at 100% power output. The chopped stocks make CNC programming less complicated. Parts can be milled directly from the acrylic sheet if a laser machine is unavailable.

CNC milling

A milling machine is needed to create the parts for the tank manifold (2 pieces), cartridge manifold (2 pieces), and sample cartridges. Use the Autodesk Fusion360 program to generate the toolpaths and G-codes for the milling machine. Machine all the parts in the STEP folder for assembly.

Gasket fabrication

RTV 615 (Momentive) is used to make the gasket. Part A and part B should be mixed in a 10:1 ratio before being poured into the bottom piece of the cartridge manifold (part B2). To cure, bake the mixture for two hours at 80 °C.

Drilling/Tapping

Create the mounting threads for solenoid valves and pneumatic fitting connectors. The detailed tap sizes are shown in Fig. 5(A). Taps enter from the closer side. Before tapping, a 2 mm drill bit needs to be used to drill the hole in the air tank tube.

Bonding/gluing

Use diffusion bonding to make the tank manifold and cartridge manifold by combining two separate pieces into a single unit [22]. Align and place the manifolds in a heat press, then apply heat at 120 °C from both sides for 30 min. Apply superglue to seal one side of the air tank tube with a 19 × 19 mm acrylic piece and bond the other side to the tank manifold. Fig. 3 and Fig. 4 depict how the manifolds and tanks are laid out.

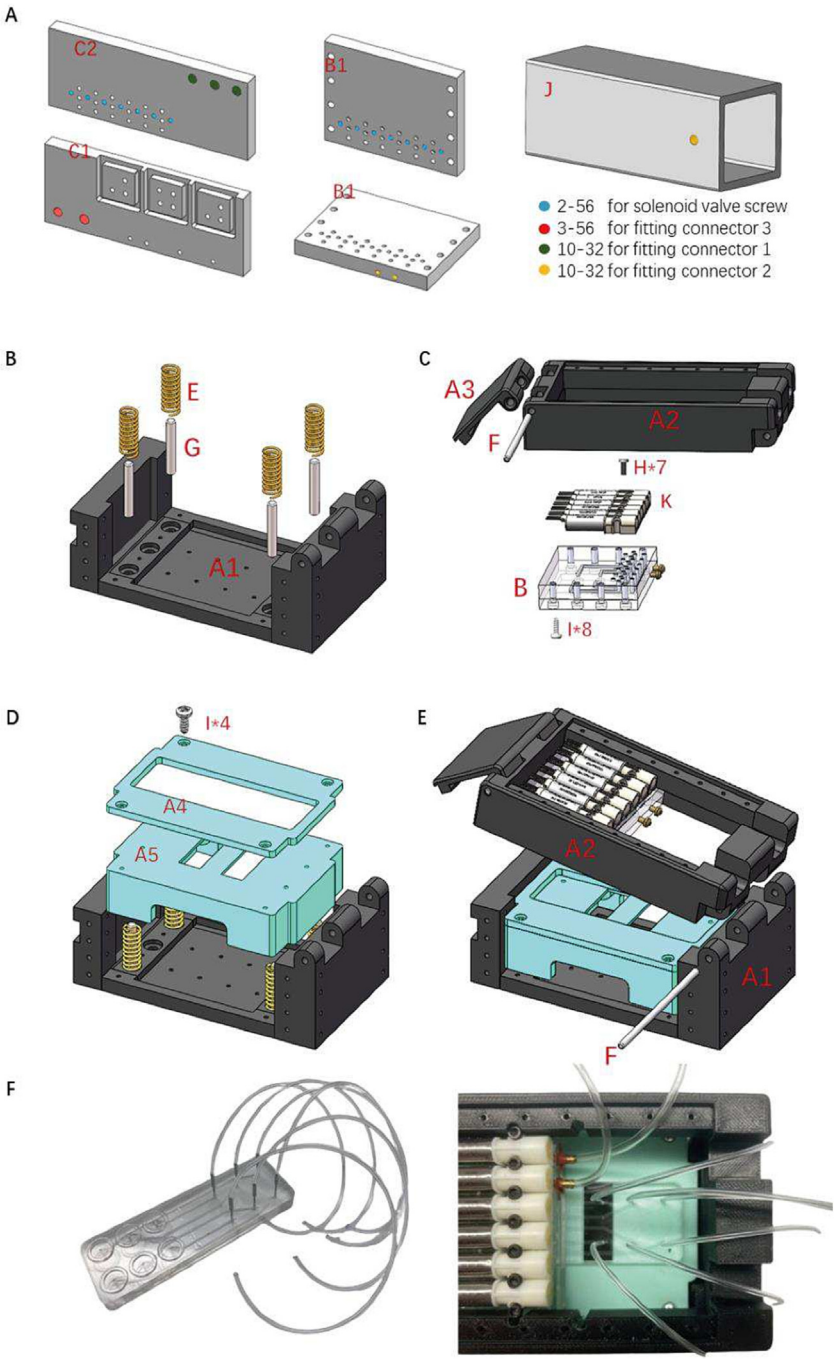

Fig. 5. Mechanical assembly guide. (A) Drilling and tapping (B) Base holds the 4 mm rod and die spring. (C) Screw the solenoid valves on the cartridge manifold, then attach the cartridge manifold to the cover. Join the cover and the cover lock with a 3 mm rod. (D) Screw the positioner on the spring stage. Then fit the stage into the base. The stage will be supported by the springs. (E) Join the assembled cover and base with a 3 mm rod. (F) The adapter cartridge can turn the system into a general-purpose pressure source with six output ports. Insert six 22-gauge needles into the output ports of the cartridge. Use silicone tubing with proper inner diameter to connect the system to external microfluidic chips. Parts are labeled as follows: A1-Base, A2-Cover, A3-Cover lock, B1–Top piece of cartridge manifold, C1-Tank side piece of tank manifold, C2-Valve side piece of tank manifold, E-Spring, F-3 mm rod, G-4 mm rod, H-Flat screw, I-Self tapping screw, J-Air tank, K-Solenoid valves.

Install fitting connectors

Install the proper fitting connectors on the tank manifold, cartridge manifold, and air tanks, as shown in Fig. 5(A).

Assembly

Socket structure

Step 1 (Fig. 5(B)): Place the base (part A1) on a flat surface and insert the 4 mm rods (part G) into the slots on the base. Then install the springs (part E).

Step 2 (Fig. 5(C)): Attach the cartridge manifold's six solenoid valves (part K) with seven flat screws first (part H). Connect the jumper wires on the solenoid valves before using eight self-tapping screws (part I) to secure the manifold to the cover (part A2) from the lower side. After that, join the cover and cover lock (part A3) using a 3 mm rod.

Step 3 (Fig. 5(D)): Mount the positioner (part A5) onto the spring stage (part A4) with four self-tapping screws (Part I). Then the spring stage can be located and supported by the springs through the holes under it.

Step 4 (Fig. 5(E)): Join the base (part A1) and cover (part A2) using a 3 mm rod (part F). The socket structure is ready for the assay cartridge.

Step 5 (Fig. 5(F)) (optional): If the pressure source mode is preferred, the adapter cartridge needs to be prepared by inserting six 22-gauge needles and proper tubing that fit the external microfluidic chip [13,23]. Insert the cartridge into the positioner, and the system is ready to work as a general-purpose pressure source with six output ports.

Electrical wiring and pneumatic tubing connection

In the arrangement shown in Fig. 6, connect the solenoid valves on the tank manifold to ports A–F and the solenoid valves on the cartridge manifold to ports 1–6. Connect port 8 to the pump. Connect the 12 V power rail from the battery to the 12 V port on the PCB. The polarity for each port is documented in the pressurecontroller.hpp file in the firmware file. Connect the air tanks to the pressure sensors using the 1/16″ tubing. Connect the pump, check valve and the tank manifold using 3/32″ tubing. The cartridge manifold should be attached to the appropriate output ports of the air tanks with 1/16″ tubing. In the demonstrated configuration, the input port for solenoid valves 1–5 is connected to the output port of P2, and the input port for solenoid 6 is connected to the atmosphere.

Four I^2C ports and three additional power rails are provided for extension. Additional devices, such as sensors, heating elements, wireless communication modules, could be added to the system through these ports.

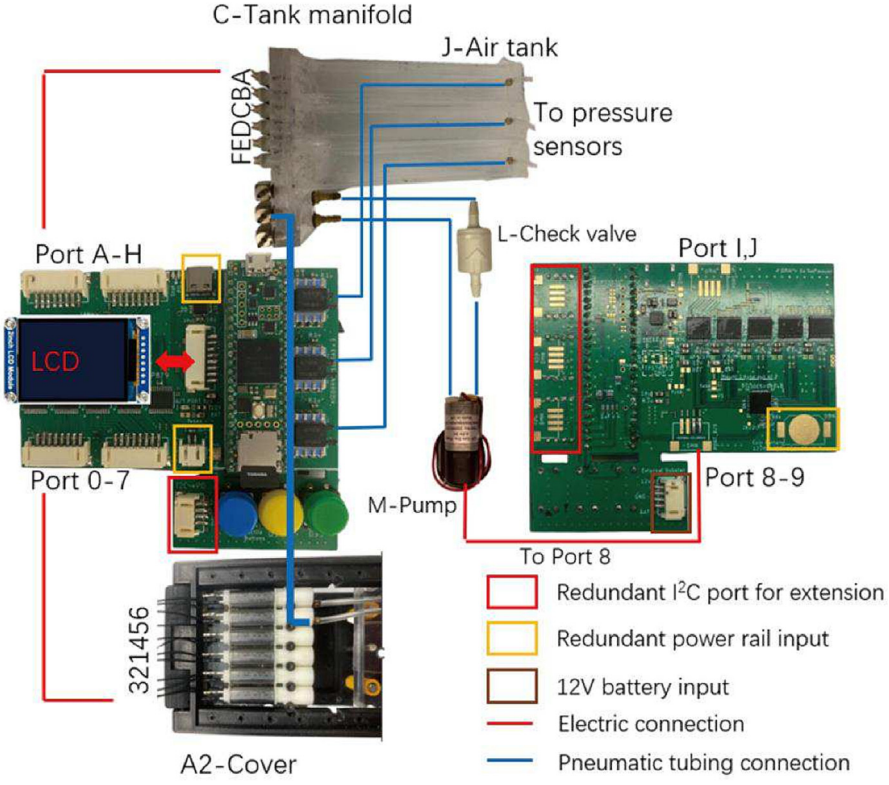

Fig. 6. Electric and pneumatic connection. The LCD and solenoid valves are connected to the ports on the top side of the PCB. The pump and 12 V input from the battery is connected to the connectors on the bottom side of the PCB. The input port of the pump is connected to the air tank 3. The output port of the pump is connected to air tank 1 after going through a check valve. The three controlled air tank outputs should be connected to the air input ports on the cartridge manifold. P2 was connected to the input port for valve 1–5 for the illustrated test and experiment. Redundant I^2C port and power rail inputs can be used for system extension with additional devices.

Operation instructions

Step 1: Open the firmware using Visual Studio Code software and the PlatformIO extension. Then upload the firmware to the Teensy board. Detailed documentation for this step can be found on the PlatformIO website for the Teensy platforms [24].

Step 2: Load the Lua script files into a microSD card, then insert the microSD card into the Teensy board.

Step 3: Connect the 12 V and USB port on the battery to the 12 V port on the PCB and the micro-USB port on the Teensy board. Then switch on the battery to power the system.

Step 4: Insert the cartridge into the system. Then lock the cover and push the green button to choose the sample Lua script file. The commands in the script will then be executed automatically to carry out the work.

Optional: In step 3, connect the Teensy board to a PC instead of the battery. Then commands can be sent using any serial port control program (e.g., PlatformIO terminal, Arduino serial monitor, PuTTY). This feature can be used to troubleshoot, debug, and manually control the system in real-time.

Validation and characterization

Pressure stabilization performance

A series of characterizations of the pneumatic performance were performed. The achievable pressure range of air tank 1 and 2, the leakage rate of air tank 1, and the pressure stability of the air tanks were tested. The tests were conducted under the most duty-intensive scenario: a bottom-sealed sample assay cartridge without reagents, where the solenoid valves on the air tank manifold and the pump will be activated most frequently. The open frequency of the solenoid valves on the cartridge manifold was configured at once per 30 s to match the SARS-CoV-2 spike antibody immunoassay demonstrated below. The maximum achievable pressure was 5.8 psi (40 kPa), which could be improved by changing to a more powerful pump. The pressure range setting for the air tank was 1–1.6 psi (6.89–11 kPa), while air tank 2 was set to 0.2–0.22 psi (1.38–1.52 kPa).

The test results in Fig. 7 show that it took about 2.6 s for the pump to increase the pressure in air tank 1 to 1.6 psi (6.89–11 kPa) and 0.7 s for pressure in air tank 2 to reach 0.24 psi (1.65 kPa) by activating a solenoid valve to deliver air from air tank 1. The starting pressure was not 0 since the test was done right after a previous test to simulate a continuous working situation.

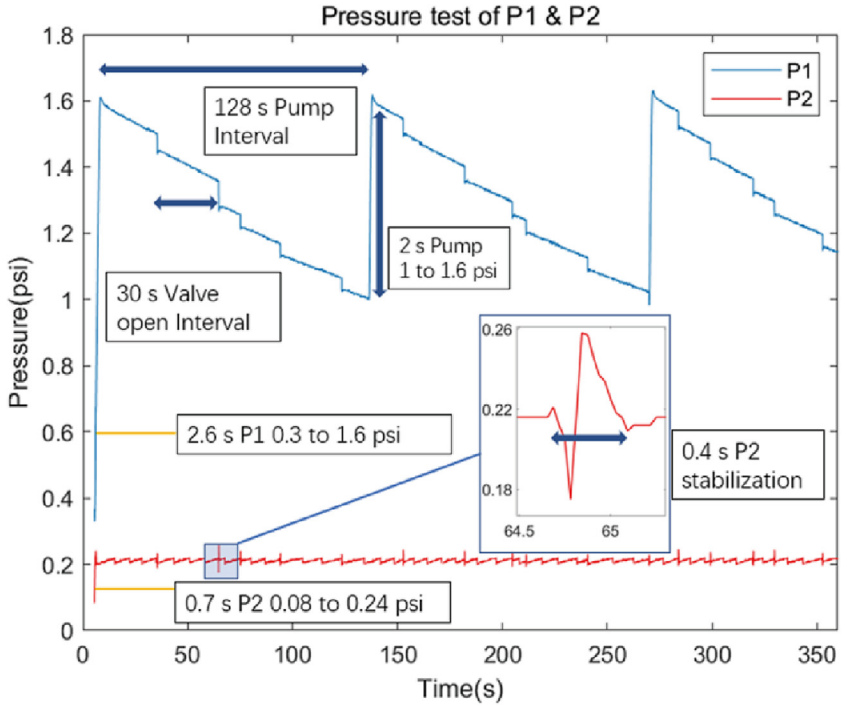

Fig. 7. Pneumatic performance test. P1 was set to 1–1.6 psi (6.89–11 kPa). P2 was set to 0.2–0.22 psi (1.38–1.52 kPa). One solenoid valve on the cartridge manifold, which was connected to P2, was opened for 50 ms every 30 s to simulate the SARS-CoV-2 spike antibody immunoassay. The test lasted for 360 s. The system achieved the programmed pressure levels in 1.6 s. The stabilization time for P2 was 0.4 s.

A pressure drop on the P1 line was observed every 30 s, which matched the solenoid valve's open interval. A steep rise to around 0.26 psi (1.79 kPa) was observed at the same time when the P1 dropped to increase P2 through a solenoid valve on the air tank manifold. The sudden change can be stabilized to the target range in 0.4 s. Although a slow leakage from air tank 1 to air tank 2 led to the 'air tank 2 to the atmosphere' solenoid valve being switched around every 8 s to stabilize the pressure in air tank 2, the pressure levels of the two air tanks were maintained in range.

In this test condition, P1 dropped from 1.6 psi (11 kPa) to 1 psi (6.89 kPa) in around 128 s, and then the pump restored the pressure to 1.6 psi (11 kPa) in 2 s. Improving the sealing of the pneumatic subsystem could improve performance and reduce power consumption.

SARS-CoV-2 spike antibody immunoassay

A bead-based SARS-CoV-2 anti-spike IgG antibody fluorescence immunoassay (FIA) was conducted on the sample cartridge (Fig. 8 (A-C)) as a demonstration of the system. Two 6.35 mm diameter hemisphere (67 uL) reservoirs for reagent 1 and reagent 2 are located on the top side of the cartridge; a 490 uL reservoir for reagent 3 and an 860 uL waste reservoir are on the bottom side of the cartridge. A series of 0.4 mm hemisphere channels were milled on the bottom side of the cartridge for reagents to flow at a precise flow rate. A vertical via hole was drilled in every reagent reservoir to provide a path for air and reagents. Three buffering channels (1.2 mm width, 1 mm height) were inserted between the flow channels and each reagent reservoir to provide error tolerance and prevent undesired reagent flow into the flow channel. A 1.5 mm diameter, 0.3 mm height beads chamber where all reactions happen was placed at the end of the flow channel. Six O-rings on the top of the cartridge provide alignment to the cartridge manifold and improve air tightness. The prepared beads and reagents were loaded into the cartridge with a pipette. The information about the reagents, cartridge preparation, and assay protocol can be found in the supplementary document.

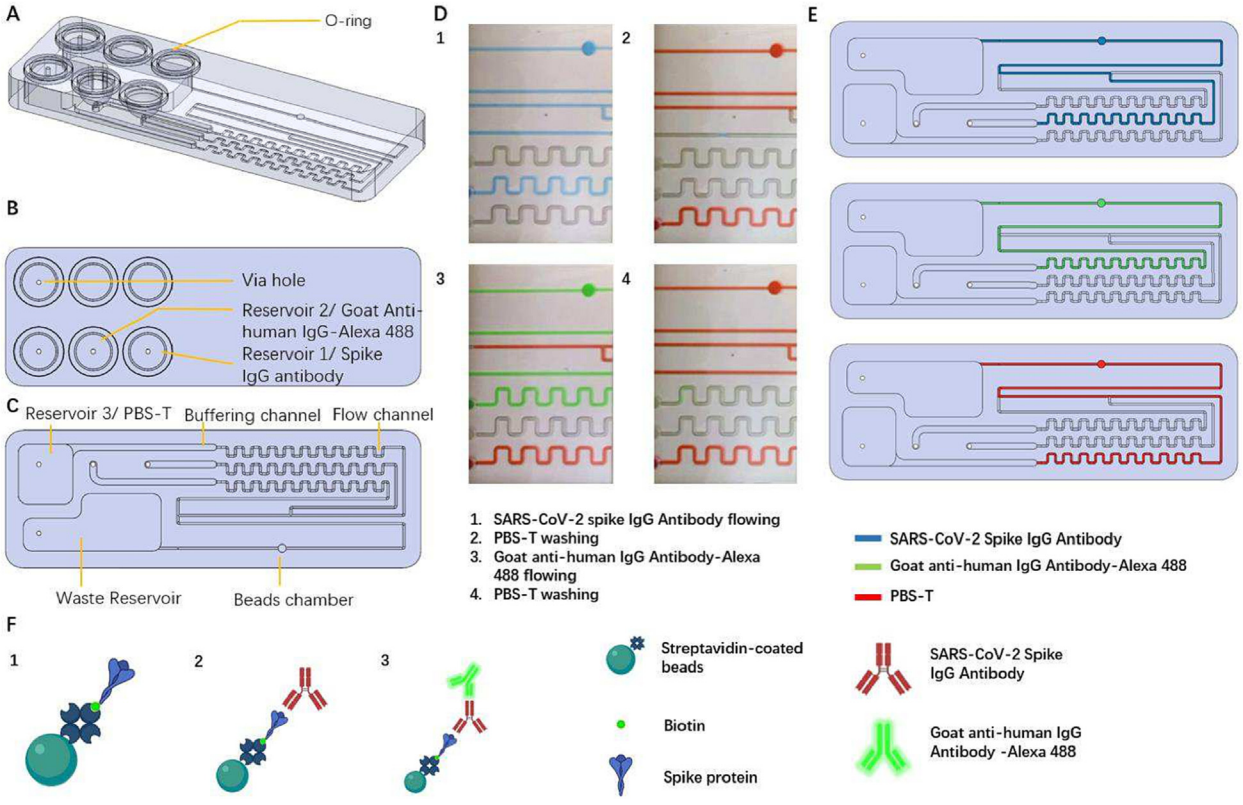

Fig. 8. A bead-based SARS-CoV-2 spike antibody immunoassay on the sample cartridge. (A) Isometric view of the cartridge with one O-ring pointed. (B) Top view with vertical hole and hemisphere reservoirs pointed. (C) Bottom view with two non-hemisphere reservoirs, buffering channel, flow channel, and beads chamber pointed. (D)Simulated assay with food dye to demonstrate reagent switching and liquid handling. (1) Anti-spike IgG antibody (Blue) flowing (2) PBS-t washing buffer (Red) washing (3) Goat Anti-human IgG Antibody-Alexa 488 fluorescent detection antibody (Green) flowing (4) PBS-T washing buffer (Red) final washing. (E) Ideal flow paths of the reagents (top view), while the real result could be different because of air leakage and previous flow steps. (F) The schematic diagrams of the beads after (1) Spike protein functionalization (2) Spike IgG antibody bind to spike protein (3) Alexa 488 conjugated goat anti-human IgG antibody bind to Spike IgG antibody. (For interpretation of the references to colour in this figure legend, the reader is referred to the web version of this article.)

The reagent flowing procedure and routes are shown in Fig. 8 (D, E). The schematic diagrams of the beads complex for each procedure are shown in Fig. 8 (F). A slow-release method was used to flow the anti-spike IgG antibody and Goat anti-human IgG – Alexa 488 detection antibody. The open time of the solenoid valves was set to 50 ms; hence the reagent reservoirs were connected to air tanks to gain pressure for 50 ms and disconnected to stay sealed, then the pressure that just built up decreased while pushing the reagents. At every 30 s, the solenoid valve was switched on and off once during the reagent pushing period. By employing such a method, a 10-minute incubation time was achieved with 50 uL reagent. For the PBS-T washing buffer, a higher pressure was used, and the solenoid valve was always open during the flow period. The concentrations of the SARS-CoV-2 anti-spike IgG antibody solutions were 100 ng/mL, 500 ng/mL, 1 ug/mL, 2 ug/mL. Phosphate-buffered saline (PBS) was used as the negative control. The concentration of the detection antibody was 10 ug/mL. The whole assay took about 30 min to complete.

Once the assay ended, the cartridge was taken out from the system and fit into the glass slide holder for fluorescence readout on an Olympus IX71 microscope. The mean intensities of the background and beads were calculated. The net fluorescence intensity (subtract background intensity from beads intensity) result is shown in Fig. 9. The limit of detection (LoD) is 31.1 ng/mL (207 pM), which is comparable to some previously reported ELISAs (LoDs range from 25 ng/mL to 300 ng/mL) [25–28]. By using reagents that have undergone rigorous development and testing, the LoD could be further reduced.

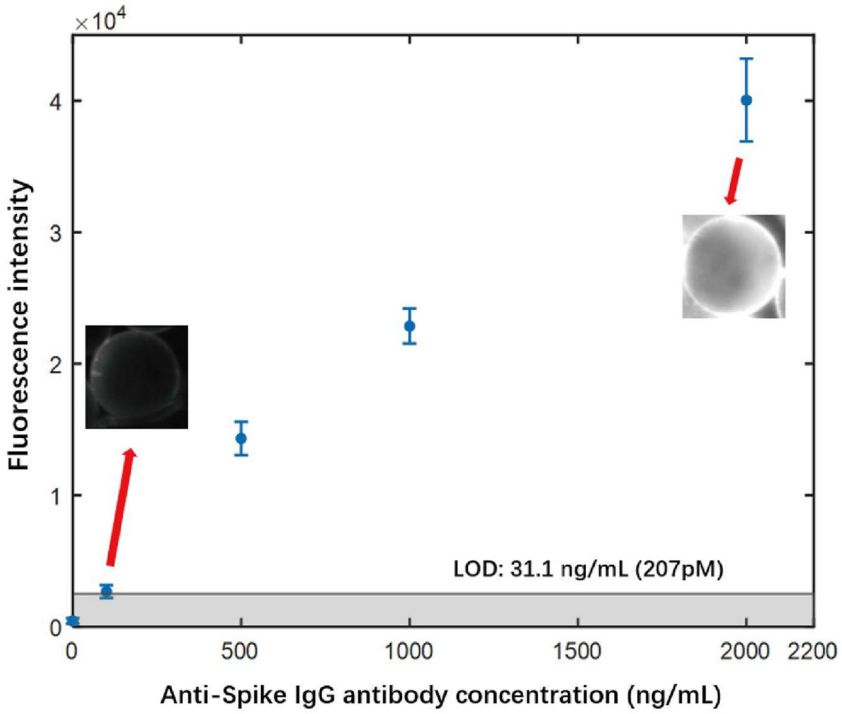

Fig. 9. SARS-CoV-2 immunoassay fluoresce intensity mean and standard deviation. 12 data points per group for the negative control, 100 ng/mL, 500 ng/mL groups,16 data points per group for 1000 ng/mL and 2000 ng/mL groups. Two bead images show results of 100 ng/mL and 2ug/mL of SARS-CoV-2 anti-spike IgG antibody. The LoD is 31.1 ng/mL (207 pM).

Discussion

The goal of this research is to develop a miniaturized plug-and-play microfluidic liquid handling automation platform. The demonstrated handheld system minimizes human operations in conventional immunoassay experiments with a small footprint and less power consumption, which makes it hand-holdable to fit into point-of-care, research laboratories, and special circumstances.

Recently, automated liquid/reagent handling systems have made advances in miniaturization and ease of use. However, most of these systems are still relatively bulky and require external power sources [16–19]. Some systems act as a controller, which requires an external pneumatic system [17,18]. Some integrated system still requires extensive liquid transferring preparation and continuous human monitoring, which might not be desired for out-of-lab usage [16]. Some systems lack regulated pressure control for liquid flowing and only allow a one-time switch for one reagent, which might narrow its applications. Also, the cartridges used in such systems require complex manufacturing processes, which may increase the test cost [19].

Table 1
Comparison of available automated microfluidic liquid handling system/module.

Platform	Type	Size/weight	External instrument requirement	Pressure control method
this work	Standalone liquid handling system	16.5 × 11.5 × 7 cm/ 801 g with battery	Self-contained, plug & play	Regulated air
MCSP [18]	Controller/driver module	9.65 × 9.65 cm/NA	Require external pneumatic system, power source, and microfluidic chip	NA
KATARA [17]	Controller/driver module	19.3 × 11.7 × 6.1 cm/ NA	Require external pneumatic system, power source, and microfluidic chip	NA
All-in-one [16]	Automated microfluidic control system	30.5 × 17.8 x8.7 cm/ NA	Require external power source, microfluidic chip	Regulated air
Hu, et al [19]	Standalone immunoassay system	33 × 19 × 19 cm/ 4 kg	Require external power source	Pump motor speed

To address these problems, we have developed a handheld plug-and-play microfluidic liquid handling automation platform for immunoassays that is suitable for use inside and outside of a professional laboratory. Unlike robotic pipetting systems, our platform does not require complex mechanical moving parts. With a smaller footprint and lower power consumption, it is highly applicable for a wider range of application scenarios.

The demonstrated system is compared with the above-mentioned automated microfluidic liquid handling systems in terms of system type, size and weight, external instrument requirement, and pressure control method (Table 1). Also, the cost of each test is reduced by making the cartridge easy to mass-produce by injection molding.

In future work, the cross-contamination between cartridge to cartridge should be rigorously evaluated. Comprehensive investigation and verification should be done to ensure there is no cross-contamination. A miniaturized fluorescence (or chemiluminescence or absorption) readout module could be integrated to upgrade this liquid handling system into a self-contained, automated immunoassay device and potentially support actual point-of-care operations.

Conclusion

We have demonstrated a fully automated, modularized, cartridge-based plug-and-play handheld microfluidic liquid handling system. With appropriate cartridge design and modification, the system could accommodate types of immunoassays or work as a stand-alone microfluidics pressure source [29–31]. Beyond COVID-19, there are applications that require highly sensitive and quantitative assays, such as cardiac Troponin tests for heart attack detection. In addition, automated liquid handling can be used in many analytical assays, such as qPCR, sequencing, and flow cytometry.

The demonstrated system can minimize human operations in the widely used immunoassays and other microfluidic experiments with a small footprint and low power consumption, which makes it handheld to serve applications from point-of-care diagnostics to basic biomedical research.

Ethics statements

No human or animal studies were conducted in this work.

Declaration of Competing Interest

The authors declare that they have no known competing financial interests or personal relationships that could have appeared to influence the work reported in this paper.

Acknowledgments

This work was supported by the National Institutes of Health grant 1U01EB021986-01.

Appendix A. Supplementary data

Supplementary data to this article can be found online at https://doi.org/10.1016/j.ohx.2023.e00420.

References

[1] T.G. Henares, F. Mizutani, H. Hisamoto, Current development in microfluidic immunosensing chip, Anal. Chim. Acta 611 (2008) 17–30, https://doi.org/10.1016/j.aca.2008.01.064.
[2] D. Wild (Ed.), The Immunoassay Handbook: Theory and Applications of Ligand Binding, ELISA, and Related Techniques, 4th ed., Elsevier, Oxford; Waltham, MA, 2013.
[3] R.M. Lequin, Enzyme Immunoassay (EIA)/Enzyme-Linked Immunosorbent Assay (ELISA), Clin. Chem. 51 (2005) 2415–2418, https://doi.org/10.1373/clinchem.2005.051532.
[4] Opentrons | Open-source Lab Automation, starting at $5,000 n.d. https://opentrons.com/ (accessed May 20, 2022).

[5] Automated Single-Use Systems | Parker NA n.d. https://ph.parker.com/us/en/automated-single-use-systems (accessed May 20, 2022).
[6] M.A. Unger, H.-P. Chou, T. Thorsen, A. Scherer, S.R. Quake, Monolithic microfabricated valves and pumps by multilayer soft lithography, Science 288 (2000) 113–116, https://doi.org/10.1126/science.288.5463.113.
[7] K.W. Oh, C.H. Ahn, A review of microvalves, J. Micromech. Microeng. 16 (2006) R13.
[8] D.J. Laser, J.G. Santiago, A review of micropumps, J Micromech Microeng 14 (2004) R35–R64, https://doi.org/10.1088/0960-1317/14/6/R01.
[9] M.G. Pollack, R.B. Fair, A.D. Shenderov, Electrowetting-based actuation of liquid droplets for microfluidic applications, Appl Phys Lett 77 (2000) 1725–1726, https://doi.org/10.1063/1.1308534.
[10] C.L. Hansen, M.O.A. Sommer, S.R. Quake, Systematic investigation of protein phase behavior with a microfluidic formulator. Proc. Natl. Acad. Sci. 2004;101:14431–6. 10.1073/pnas.0405847101.
[11] T. Thorsen, S.J. Maerkl, S.R. Quake, Microfluidic large-scale integration, Science 298 (2002) 580–584, https://doi.org/10.1126/science.1076996.
[12] D.M. Rissin, D.R. Walt, Digital concentration readout of single enzyme molecules using femtoliter arrays and poisson statistics, Nano Lett 6 (2006) 520–523, https://doi.org/10.1021/nl060227d.
[13] B. Li, L. Li, A. Guan, Q. Dong, K. Ruan, R. Hu, et al, A smartphone controlled handheld microfluidic liquid handling system, Lab Chip 14 (2014) 4085–4092, https://doi.org/10.1039/C4LC00227J.
[14] R.C. Wong, H.Y. Tse, Lateral Flow Immunoassay, Springer, New York, 2009.
[15] K.A. Addae-Mensah, Y.K. Cheung, V. Fekete, M.S. Rendely, S.K. Sia, Actuation of elastomeric microvalves in point-of-care settings using handheld, battery-powered instrumentation, Lab Chip 10 (2010) 1618–1622, https://doi.org/10.1039/C002349C.
[16] C. Watson, S. Senyo, All-in-one automated microfluidics control system, HardwareX (2019) 5, https://doi.org/10.1016/j.ohx.2019.e00063.
[17] J.A. White, A.M. Streets, Controller for microfluidic large-scale integration, HardwareX 3 (2018) 135–145, https://doi.org/10.1016/j.ohx.2017.10.002.
[18] F. Kehl, V.F. Cretu, P.A. Willis, Open-source lab hardware: a versatile microfluidic control and sensor platform, HardwareX (2021) 10, https://doi.org/10.1016/j.ohx.2021.e00229.
[19] B. Hu, J. Li, L. Mou, Y. Liu, J. Deng, W. Qian, et al, An automated and portable microfluidic chemiluminescence immunoassay for quantitative detection of biomarkers, Lab Chip 17 (2017) 2225–2234, https://doi.org/10.1039/C7LC00249A.
[20] BOXER 10KD Diaphragm Pump Series - Boxer Pumps n.d. https://www.boxerpumps.com/en/products/miniature-diaphragm-pumps-air-gas/boxer-10kd-diaphragm-pump-series/ (accessed March 26, 2023).
[21] S.M. Recktenwald, C. Wagner, T. John, Optimizing pressure-driven pulsatile flows in microfluidic devices, Lab Chip 21 (2021) 2605–2613, https://doi.org/10.1039/D0LC01297A.
[22] A. Yousefpour, M. Hojjati, J.-P. Immarigeon, Fusion bonding/welding of thermoplastic composites, J. Thermoplast. Compos. Mater. 17 (2004) 303–341, https://doi.org/10.1177/0892705704045187.
[23] T. Petreus, E. Cadogan, G. Hughes, A. Smith, V. Pilla Reddy, A. Lau, et al, Tumour-on-chip microfluidic platform for assessment of drug pharmacokinetics and treatment response, Commun. Biol. 4 (2021) 1–11, https://doi.org/10.1038/s42003-021-02526-y.
[24] Teensy — PlatformIO latest documentation n.d. https://docs.platformio.org/en/latest/platforms/teensy.html (accessed October 22, 2022).
[25] C. Klumpp-Thomas, H. Kalish, M. Drew, S. Hunsberger, K. Snead, M.P. Fay, et al, Standardization of ELISA protocols for serosurveys of the SARS-CoV-2 pandemic using clinical and at-home blood sampling, Nat. Commun. 12 (2021) 113, https://doi.org/10.1038/s41467-020-20383-x.
[26] V. Roy, S. Fischinger, C. Atyeo, M. Slein, C. Loos, A. Balazs, et al, SARS-CoV-2-specific ELISA development, J. Immunol. Methods 484–485 (2020), https://doi.org/10.1016/j.jim.2020.112832 112832.
[27] Anti-SARS-CoV-2 (COVID-19) IgG Antibody to Spike Protein S1 Quantitative Titration ELISA Assay Kit. Eagle Biosciences n.d. https://eaglebio.com/product/anti-sars-cov-2-covid-19-igg-antibody-to-spike-protein-s1-quantitative-titration-elisa-assay-kit/ (accessed February 20, 2023).
[28] SARS-CoV-2 / COVID-19 ELISA Kits | www.antibodies-online.com n.d. https://www.antibodies-online.com/areas/infectious-disease/covid-19/sars-cov-2-elisa-kits/ (accessed February 20, 2023).
[29] T. Hansson, S. Sjolander, Valve, especially for fluid handling bodies with microflowchannels. US5593130A, 1997.
[30] W.H. Grover, A.M. Skelley, C.N. Liu, E.T. Lagally, R.A. Mathies, Monolithic membrane valves and diaphragm pumps for practical large-scale integration into glass microfluidic devices, Sens. Actuators B 89 (2003) 315–323, https://doi.org/10.1016/S0925-4005(02)00468-9.
[31] Webster ME. Valve with flexible sheet member. US4858883A, 1989.

Sheng Wang received a B.Sc. in Optoelectronic Information Science and Engineering from Nankai university, China, in 2017, a M. Sc. in electrical engineering from George Washington University (GWU) in 2020. Currently, he is a PhD candidate in the Nanophotonics and Microfluidics Lab at GWU, conducting research on wearable sensors, wireless sensor network, point-of-care diagnostic devices, and microfluidics.

Baichen Li completed his master's degree in Biomedical Engineering at The George Washington University (GWU) in 2013. He worked in a medical device startup as an electrical engineer before he returned to pursue a Ph.D. degree in 2015 at GWU. He completed his Ph.D. program in 2021. Currently he is a postdoctoral researcher in Tsinghua University, China.

David McLeod received a B.Sc. in Bioengineering from Clemson University in 2019. Currently he is a PhD candidate in the Nanophotonics and Microfluidics Lab at GWU and conducts research on high-throughput microfluidic systems for use in tissue engineering and cell culture.

Zhenyu Li received a B.Sc. in precision instruments from Tsinghua University, China, in 1999, a M.Sc. in electrical engineering from University of California at Santa Barbara in 2000, and a Ph.D. in electrical engineering from California Institute of Technology (Caltech) in 2008. He then completed postdoctoral studies at the Howard Hughes Medical Institute Janelia Research Campus and Caltech. Currently he is an Associate Professor of Biomedical Engineering at The George Washington University, Washington DC with research interests including biosensors and medical devices using microfluidics, MEMS, Optofluidics and flexible electronics. He has published over 50 peer-reviewed articles and holds seven patents.